L-Arginine Binding to Liver Arginase Requires Proton Transfer to Gateway Residue His141 and Coordination of the Guanidinium Group to the Dimanganese(II,II) Center†

Sergei V. Khangulov,*,‡ Thomas M. Sossong, Jr.,§ David E. Ash,§ and G. Charles Dismukes*,‡

Department of Chemistry, Henry H. Hoyt Laboratory, Princeton University, Princeton, New Jersey 08544, and Department of Biochemistry, Temple University, School of Medicine, Philadelphia, Pennsylvania 19140

Received November 25, 1997; Revised Manuscript Received March 16, 1998

ABSTRACT: Rat liver arginase contains a dimanganese(II,II) center per subunit that is required for catalytic hydrolysis of L-arginine to form urea and L-ornithine. A recent crystallographic study has shown that the Mn_2 center consists of two coordinatively inequivalent manganese(II) ions, Mn_A and Mn_B, bridged by a water (hydroxide) molecule and two aspartate residues [Kanyo et al. (1996) *Nature 383*, 554−557]. A conserved residue, His141, is located near the proposed substrate binding region at 4.2 Å from the bridging solvent molecule. The present EPR studies reveal that there is no essential alteration of the Mn_2 site upon mutation of His141 to an Asn residue, which lacks a potential acid/base residue, while the catalytic activity of the mutant enzyme is 10 times lower *vs* wild-type enzyme. The binding affinity of L-lysine, L-arginine (substrate), and N^{ω}-OH-L-arginine (type 2 binders) increases inversely with the pK_a of the side chain. Binding of L-lysine is more than 10 times weaker, and the substrate Michaelis constant (K_m) is >6-fold greater (weaker binding) in the His141Asn mutant than in wild-type arginase. L-Lysine and N^{ω}-OH-L-arginine, type 2 binders, induce extensive loss of the EPR intensity, suggesting direct coordination to the Mn_2 center. From these data and the pH dependence of type 2 binders, we conclude that His141 functions as the base for deprotonation of the side-chain amino group of L-lysine and the substrate guanidinium group, $-NH-C(NH_2)_2^+$ and that the unprotonated side chain of these amino acids is responsible for binding to the active site. A different class of inhibitors (type 1), including L-isoleucine, L-ornithine, and L-citrulline, suppresses enzymatic activity, producing only minor change in the zero-field splitting of the Mn_2 EPR signal and no change in the EPR intensity, suggestive of minimal conformational transformation. We propose that type 1 α-amino acid inhibitors do not bind directly to either Mn ion, but interact with the recognition site on arginase for the α-aminocarboxylate groups of the substrate. A new mechanism for the arginase-catalyzed hydrolysis of L-arginine is proposed which has general relevance to all binuclear hydrolases: (1) Deprotonation of substrate L-arginine(H^+) by His141 permits entry of the neutral guanidinium group into the buried Mn_2 region. Binding of the substrate imino group (>C═NH), most likely to Mn_B, is coupled to breaking of the $Mn_B-(\mu\text{-}H_2O)$ bond, forming a terminal aquo ligand on Mn_A. (2) Proton transfer from the terminal Mn_A-aqua ligand to the substrate N^{δ}-guanidino atom forms the nucleophilic hydroxide on Mn_A and the cationic $N^{\delta}H_2^+$-guanidino leaving group. Protonation of the substrate $-N^{\delta}H_2^+$-group is likely assisted by hydrogen bonding to the juxtaposed anionic carboxylate group of Glu277. (3) Attack of the Mn_A-bound hydroxide at the electrophilic guanidino C-atom forms a tetrahedral intermediate. (4) Formation of products is initiated by cleavage of the $C^{\epsilon}-N^{\delta}H_2^+$ bond, yielding urea and L-ornithine(H^+).

L-Arginine is utilized in living cells for the biosynthesis of proteins. It is a precursor to the polyamines, used as growth factors, and a precursor to nitric oxide (NO), used for intracellular communication (*1*−*3*). L-Arginine is also a primary intermediate of the urea cycle, which allows many organisms to metabolize nitrogen-containing compounds with excretion of urea. The concentration of L-arginine in tissues is regulated by arginase, making this enzyme extremely important for a variety of biochemical reactions and biomedical applications.

Arginases from all sources require a divalent cation activator. The mammalian enzyme can be activated by Mn(II), Co(II), Ni(II), Fe(II), and Cd(II), although the physiological activator is Mn(II) (*4*, *5*). Rat liver arginase is a homotrimeric enzyme (*6*, *7*), containing one binuclear Mn(II) center, Mn_2(II), in each subunit (*8*) that is required

† This research was supported by the National Institutes of Health, Institute of Digestive Diseases and Kidney, Grants DK45414 (G.C.D.) and DK44841 (D.E.A.).

* Address correspondence to S.V.K. at fax, (609) 258-1980; e-mail, khang@chemvax.princeton.edu. Address correspondence to G.C.D. at phone, (609) 258-3949; fax, (609) 258-1980; e-mail, dismukes@chemvax.princeton.edu.

‡ Princeton University.

§ Temple University.

S0006-2960(97)02874-2 CCC: $15.00
Published on Web 05/21/1998

Scheme 1: Schematic View of Coordination of Mn Ions in the Active Center of Rat Liver Arginase Based on the 2.1 Å Resolution X-ray Structure of the Resting Enzyme[a,b]

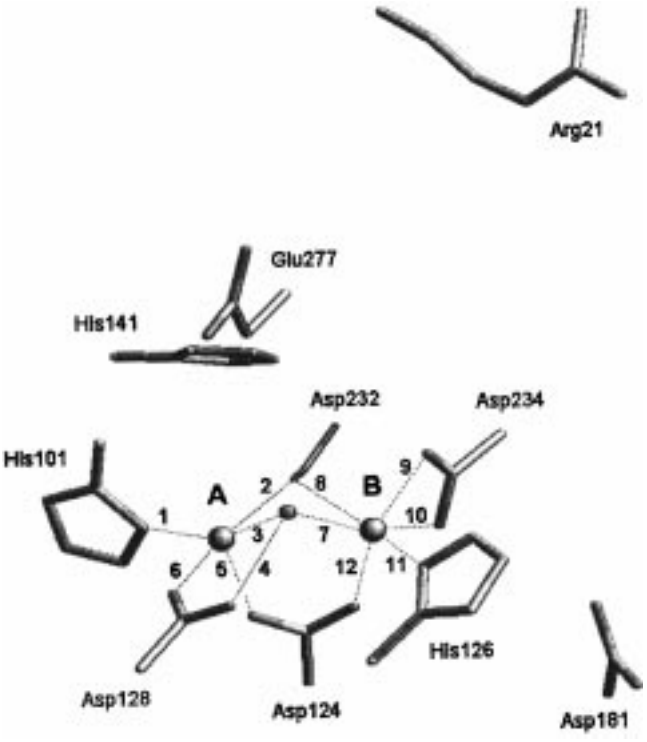

[a] The cluster includes Mn_A(II) and Mn_B(II) ions coordinated to His101 and His126 residues, respectively. Arg21 and Asp181 were proposed to bind the charged carboxyl and α-amino group of L-arginine, respectively. Glu277, located 4.5 Å away from the Mn_A center, was proposed to make a salt link to the positively charged guanidinium group of substrate L-arginine, while His141 was proposed to serve as a proton shuttle in catalysis (*7*). [b] The distances between atoms (Å): 2.24 (1), 2.29 (2), 2.36 (3), 2.81 (4), 2.02 (5), 2.12 (6), 2.41 (7), 2.45 (8), 2.10 (9), 2.30 (10), 2.08 (11), 2.05 (12).

for catalyzing the hydrolysis of L-arginine (eq 1):

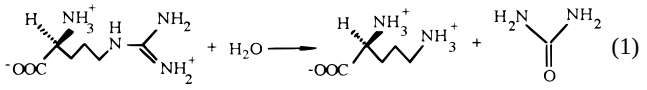

A recent study of the inhibition of liver arginase by different N^{ω}-hydroxyamino-α-amino acids suggests that three regions of the protein are critical for L-arginine hydrolysis (*9*). The "hydrolysis site" includes the binuclear Mn_2(II) center. The charged "L-α-amino acid site" is responsible for "anchoring" of the charged carboxyl group and the α-amino group of the L-arginine molecule. The "hydrophobic site" provides a proper orientation of the L-arginine side chain, placing the guanidinium group in close proximity to the Mn_2 site.

A recent 2.1 Å resolution X-ray diffraction map of the uninhibited form of rat liver arginase (*7*), as given in Scheme 1, reveals that the Mn_2 cluster is located about 15 Å from the surface of the protein. The cluster includes Mn_A(II) and Mn_B(II) ions coordinated to His101 and His126 residues, respectively. The Mn_A ion is five-coordinate and thus could be imagined either to function in substrate binding or to activate a bound water molecule by ionization to the hydroxide anion. An "L-α-amino acid recognition site"

Scheme 2: Proposed Mechanism for L-Arginine Hydrolysis by Arginase Based on Crystallographic Study of the Free Enzyme (*7*)

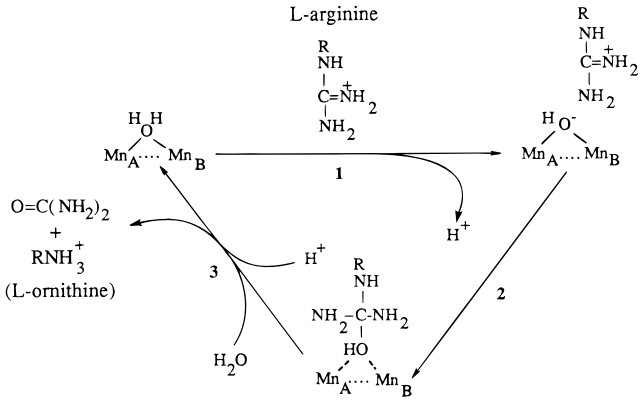

(anchoring site) was proposed to include two polar residues, Arg21 and Asp181, which may bind the charged carboxyl and α-amino group of L-arginine, respectively. The position of substrate L-arginine was not established crystallographically, but was modeled using the free enzyme coordinates. Glu277, located 4.5 Å away from the Mn_A center, was proposed to make a salt link to the positively charged substrate guanidinium group, thereby orienting the guanidinium carbon into a position favorable for nucleophilic attack by the bridging hydroxide. Direct coordination of the α-carboxylate group of the product L-ornithine to the Arg21 residue was recently demonstrated (*10*).

The main features of the mechanism proposed on the basis of the X-ray structure are given in Scheme 2. They are (1) The charged guanidinium(H^+) group of L-arginine binds to the carboxylate anion side chain of Glu277, and the μ-aquo ligand is ionized to μ-hydroxide upon substrate binding. (2) The μ-hydroxide attacks the guanidino carbon to form a triply-bridging μ_3-oxo adduct, following proton transfer from μ_3-hydroxide to substrate N^{δ} H *via* Asp128. (3) The next step is an additional proton transfer to form L-ornithine(H^+) and urea followed by product release and regeneration of the native state.

A thermodynamically plausible feature of this mechanism is the use of the second metal site for further lowering the pK_A for proton ionization from 10.6 to as low as *ca.* 7.2 for a bridging water molecule (*11*). This role has been suggested for a number of dimetallo-hydrolases (*11*, *12*). There are also three unexpected features of this mechanism: no direct role for either Mn(II) ion in substrate binding is invoked; no role for His141, located 4.2 Å from the metal-bridging solvent molecule, was proposed (it was assumed to function only as a transient proton shuttle); the proposed μ-hydroxide bridge is invoked as the nucleophile which attacks the guanidino carbon to form a trivalent μ_3-oxo bridge, even though hydroxides that bridge between two electropositive metal centers are predicted to be ineffective nucleophiles due to stabilization by the metal ions (*13*).

Wild-type arginase also catalyzes the disproportionation of hydrogen peroxide, although at a rate *ca.* 10^5 slower than Mn catalases (*14*). The presence of an intact Mn_2(II,II) center is essential for both L-arginine hydrolysis and H_2O_2 decomposition. Both the His101Asn and His126Asn mutants, which are ligands to Mn, have decreased Mn content of about 3 Mn/trimer and exhibit neither catalase nor

hydrolytic activity (*14*, *15*). Mutation of His141 to Asn produces no change in the Mn content or the catalase activity, but decreases the hydrolytic activity by 10-fold.

Herein, we have employed variable-temperature EPR measurements to test how the mutation His141Asn influences the coordination-sensitive zero-field splitting (D) and the intermanganese electron spin exchange interaction (J) of the Mn_2 center, and to evaluate the nature of the interaction with a variety of L-amino acid inhibitors. EPR reveals a flexible Mn_2 site that undergoes cleavage of the solvent bridge during the catalytic process that was not apparent from the X-ray structure.

MATERIALS AND METHODS

Rat Liver Arginase. The replacement of the conserved histidine residues His 101, His126, and His141 by Asn was performed as described by Cavalli et al. (1994). Purification of recombinant rat liver arginase was performed as described previously (*15*). Wild-type arginase and mutant enzymes were stored as crystalline precipitates in 80% saturated ammonium sulfate at 4 °C. To prepare EPR samples, an excess of ammonium sulfate was removed by centrifugation in Centricon-10 concentrators against 25 mM Hepes−KOH buffer, pH 7.5; otherwise, the pH values are indicated in the text or in the corresponding figure legends. The EPR samples contain about 100 μL of concentrated enzyme solution (3−6 mg/mL).

EPR Spectroscopy. X-band EPR spectra were obtained at 9.46 GHz on a Bruker ESP-300 spectrometer as previously described (*16*).

Temperature Dependencies of the EPR Signals. The methods used for estimation of the Mn−Mn separation, r(Mn−Mn), and the intermanganese exchange interaction ($-2JS_1S_2$) in Mn_2 enzymes are essentially identical to our previous work (*17*). The general procedure involves deconvolution by multicomponent analysis, using eq 2, of the field- and temperature-dependent Mn_2 EPR signal, $Mn_2(H,T)$, into temperature-independent excited triplet and quintet state spectra, $e_{S=1}(H)$[1] and $e_{S=2}(H)$, as a function of temperature:

$$Mn_2(H,T) \approx [\eta_1(T)e_{S=1}(H) + \eta_2(T)e_{S=2}(H)]TP^{-1/2} \quad (2)$$

where H and P are the external magnetic field and microwave power, respectively. The coefficients $\eta_1(T)$ and $\eta_2(T)$ contain all of the temperature dependence and were fit to Boltzmann population coefficients, $n_1(T)$ and $n_2(T)$, for the singlet and quintet states, respectively. The Boltzmann coefficients were calculated using an energy diagram for two Mn(II) ions, coupled by Heisenberg spin−exchange interaction, $H = -2J(S_AS_B)$ with $S_A = S_B = {}^5/_2$. The line shape of the spectrum, e_i, depends on the zero-field spitting value, $D_{S=i}$. For the quintet state, the $D_{S=2}$ value was estimated from the position of the highest field resonance peak of each spectrum (H_{hf}), based on the linear dependence of $D_{S=2}$ *versus* H_{hf} (*18*). The value of D_2 was determined by obtaining the best correspondence between the peaks and turning points of the experimental derivative spectrum and the theoretical spectrum predicted using the Baranowski diagram (D_2 *vs* resonance field diagram) as we described in detail in Figure 7 of ref (*17*). According to this diagram, there are six EPR resonances that are predicted, including their line shape. Once this is done, the most accurate determination of D_2 can be made from the position of the highest field peak, since this transition exhibits the strongest magnetic field dependence and does not overlap with other transitions. The Mn−Mn separation was estimated using a linear correlation diagram for $D_{S=2}$ *vs* r(Mn−Mn), derived from five Mn_2(II,II) model complexes (*17*).

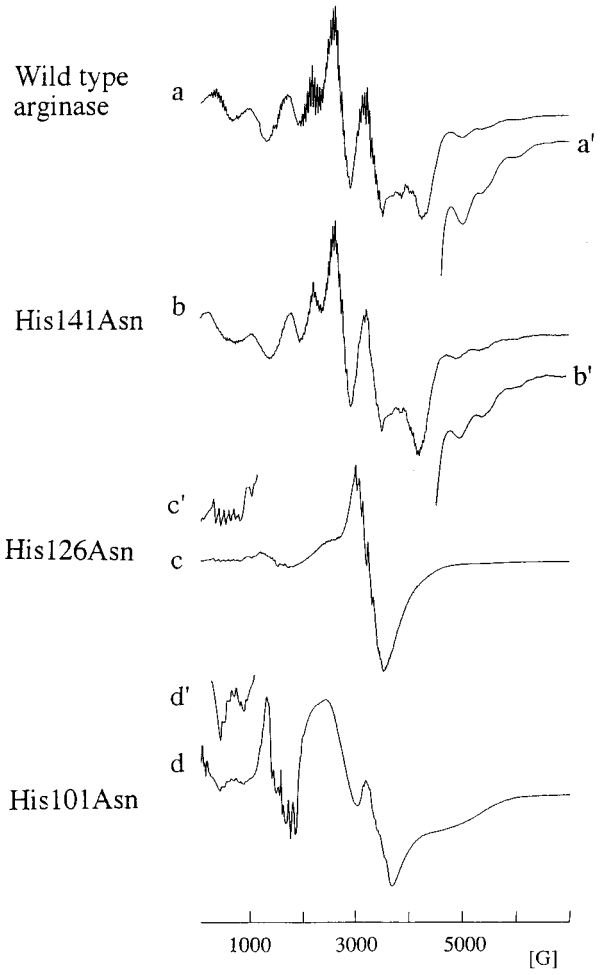

FIGURE 1: Low-temperature EPR spectra of wild-type arginase (a), His141Asn mutant (b), His126Asn mutant (c and c′), and His101Asn mutant (d and d′). Spectra were recorded at 14.0, 15.6, 16.0, and 17.0 K, respectively, and microwave power 1.61 mW. Inserts a′, b′, c′, and d′ are expansions of the spectra. Each sample contains about 100 μL of enzyme solution (28−36 mg/mL) in 50 mM HEPES, pH 7.0. The samples were prepared by washing against chelator EDTA and contained 6 Mn/trimer (a and b) and 3.6 Mn/trimer (c and d).

RESULTS

Wild-type arginase and the His141Asn mutant contain exclusively a binuclear type, Mn_2(II) center (Figure 1). Characteristic EPR parameters of these signals are given in Table 1.

EPR spectra of the His126Asn and His101Asn mutants, containing predominantly mononuclear Mn_1(II) centers, are

[1] Abbreviations: Mn_2(His141Asn) and Mn_2(wt), Mn(II)-binuclear centers and EPR signals in His141Asn mutant enzyme and wild-type arginase, respectively; $e_{S=i}$ and $D_{S=i}$, EPR signal and zero-field splitting values of paramagnetic species with spin state i = 1, 2, ..., 5, respectively; H_{hf}, magnetic field corresponding to the highest field peak of the quintet EPR signal.

Table 1: EPR Properties of the Mn_2(II,II) EPR Signals of Wild-Type Arginase and the His141Asn Mutant

property	enzyme	
	wild-type	His141Asn
$\|D_2\|$[a] (cm^{-1})	0.055, 0.067, 0.104	0.05, 0.066, 0.104
r(Mn−Mn)[b] (Å)	3.6, 3.5_5, 3.4	3.6, 3.5_5, 3.4
J[c] (cm^{-1})	-2.0 ± 0.5	-2.5 ± 0.5

[a] Zero-field splitting of quintet spin state. [b] Mn−Mn separation. [c] Exchange integral, $H = -2J(S_1S_2)$, estimated based on non-Curie temperature dependencies of the Mn_2(II,II) EPR signals.

also included in Figure 1 for comparison (spectra c and d, respectively). A detailed characterization of the EPR properties of these mutants will be discussed in another publication (*19*).

No Alteration of the Mn_2 Site Occurs upon Mutation of His141 to an Asn Residue. The EPR signal of the wild-type arginase, Mn_2(wt) (Figure 1, a), has been reported and analyzed previously (*8*, *17*).

The EPR spectrum of the His141Asn mutant signal, Mn_2-(His141Asn), is very similar to the wild-type arginase signal (Figure 1, a and b). The defining features of these Mn_2 signals include extensive ^{55}Mn hyperfine structure with average splitting (42−47 G) equal to half the value observed for monomeric manganese, a large spectral breadth extending over 6000 G due to zero-field splitting, and a non-Curie temperature dependence of the EPR intensity. We showed previously that wild-type arginase contains a pair of Mn(II) ions spin-coupled by a weak, antiferromagnetic exchange interaction, $J \approx -2.0$ cm^{-1}. The center has a diamagnetic singlet ground state ($S = 0$) and EPR-detectable triplet and quintet spin states, $S = 1$ and $S = 2$. Similar to the wild-type arginase, the temperature-dependent Mn_2(His141Asn) EPR signal, detected under nonsaturated conditions, is a superposition of two temperature-independent spectra, $e_{S=1}$-(H) and $e_{S=2}(H)$, attributed to triplet and quintet states, respectively, and shown in Figure 2, c and b.

The contribution of the triplet and quintet state signals to the observed signal at any temperature, Figure 2, a, is expressed entirely by coefficients $\eta_1(T)$ (open triangles, △) and $\eta_2(T)$ (closed circles, ●) which fit well to the predicted Boltzmann populations $n_{S=1}(T)$ and $n_{S=2}(T)$ calculated for a Mn_2(II,II) pair using a simple Heisenberg spin exchange interaction with $J = -2.5$ cm^{-1} (Figure 3).

The temperature dependencies of the quintet state EPR signal in wild-type arginase and the His141Asn mutant are indistinguishable, as shown in Figure 3, indicating that the substitution of the His141 residue for Asn does not produce a substantial change of the J value.

We have previously demonstrated that all of the major ZFS peaks are predicted by the standard magnetic dipole transition probability expression $\sim|\langle S,M|\mu_X H_{1X}|S,M'\rangle|^2$ (*17*). The positions of the resonance peaks allow an accurate estimation of the axial ZFS parameter $D_{S=2}$, which in turn yields an estimated Mn−Mn distance (Materials and Methods). For the His141Asn mutant, two distances of 3.61 and 3.55 Å are indicated by the resolution of the high-field transition into two components at field positions 5000 and 5440 G (see arrows inserted in Figure 2, b). A weak third ZFS peak may be resolved at 6000 G, corresponding to a Mn−Mn distance of 3.4 Å. The positions of all the major

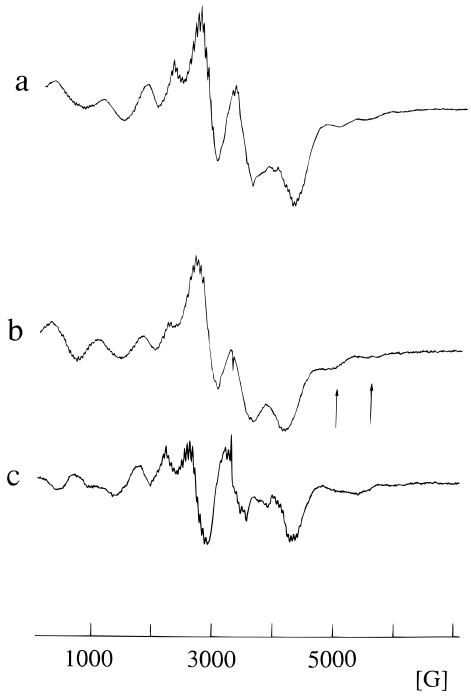

FIGURE 2: Spectrum a is the Mn_2 EPR signal of the His141Asn mutant. This temperature-dependent signal is a superposition of two temperature-independent spectra, e_1 (spectrum c) and e_2 (spectrum b), attributed to the excited triplet state ($S = 1$) and the quintet state ($S = 2$), respectively (see text). EPR conditions for spectrum a: $T = 21$ K; $P = 2.5$ mW; enzyme concentration 36 mg/mL.

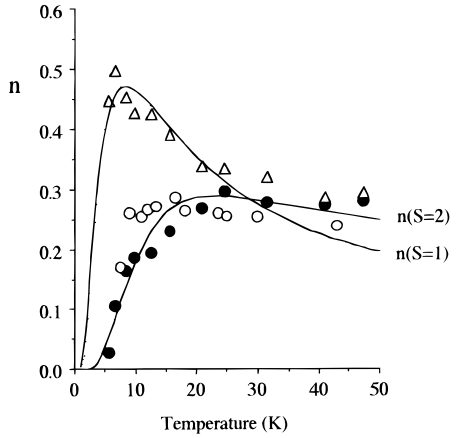

FIGURE 3: Temperature dependencies of the population coefficients η_1 (△) and η_2 (●) assigned to the contributions from the $e_{S=1}$ (triplet) and $e_{S=2}$(H) (quintet) EPR signals for Mn_2(His141Asn) (see eq 2). Open circles (○) are the temperature dependence of the Mn_2(II,II) EPR signal of wild-type arginase; the amplitude of the signal was normalized to fit the quintet state $n_2(T)$ curve. Solid lines are the predicted Boltzmann populations of the excited triplet and quintet states calculated for a pair of antiferromagnetically coupled Mn(II) ions ($J = -2.0$ cm^{-1}).

peaks and, therefore, the Mn−Mn distances are indistinguishable from those found for wild-type arginase (compare Figure 1, spectra a′ and b′).

Effect of Inhibitors and L-Arginine. Two different spectral effects can be observed on the Mn_2(wt) signal upon addition of various inhibitors of arginase activity (*14*).

(A) Type 1 Inhibitors. L-Ornithine, L-citrulline, L-isoleucine, borate [$B(OH)_3$], and hydroxylamine (NH_2OH) induce the same minor transformation of the line shape of the Mn_2(wt) EPR signal, without appreciable change in intensity.

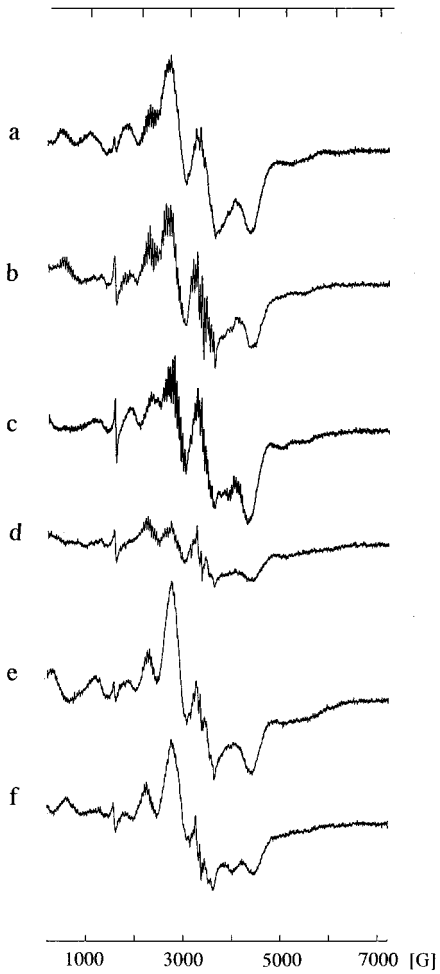

FIGURE 4: Effect of different inhibitors on the Mn_2(wt) EPR signal: control (a); in the presence of 4.0 mM L-ornithine (b); 1.2 mM L-citrulline (c); 3.0 mM L-lysine (d). In traces e and f, the Mn_2 signal from d that is suppressed by 3.0 mM L-lysine is restored by 1.8 mM isoleucine (e) and 2.2 mM borate (f). EPR conditions: $T = 22$ K; $P = 3.2$ mW; enzyme concentration 3.7 mg/mL.

This indicates that neither the zero-field splitting nor the inter-manganese exchange coupling is appreciably affected.

(B) Type 2 Inhibitors. By contrast, addition of L-lysine or N^{ω}-OH-L-arginine induces "disappearance" of the EPR signal. The disappearance is not related to redox transformation of the Mn center, since no optical absorption for Mn(III) or Mn(IV) could be observed, but rather is due to broadening of the Mn(II) EPR signals. This effect is reversible upon removal of the inhibitor by dialysis.

(a) Inhibition by L-Ornithine, L-Lysine, and L-Citrulline. L-Ornithine and L-lysine are competitive inhibitors of rat liver arginase with K_i values of 0.4−1.0 mM (*20*, *21*). Addition of a saturating amount of L-ornithine (4.0 mM) to a solution of the wild-type arginase changes the line shape but not the intensity of the Mn_2(wt) signal, replacing it with a similar, binuclear Mn_2-type EPR signal shown in Figure 4, b.

The same effect is observed with 1.2 mM L-citrulline (Figure 4, c). Although the K_i-value for L-citrulline is not available, our EPR data indicate that its K_d is about 1.0 mM. Both the L-citrulline- and L-ornithine-induced Mn_2 EPR signals (Figure 4, b and c) exhibit more extensively resolved ^{55}Mn hyperfine splittings (40−45 G), loss of one or the other of two low-field transitions (between 100 and 1500 G), and

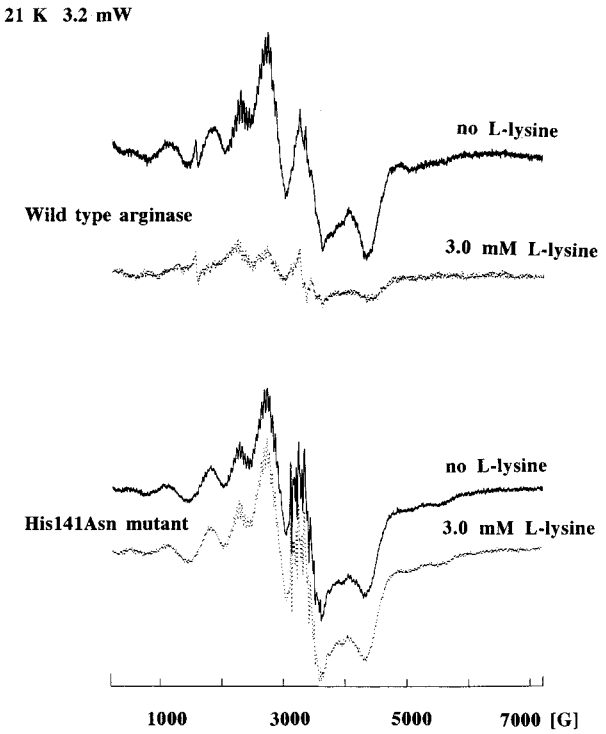

FIGURE 5: EPR spectra of wild-type arginase (top) and His141Asn mutant (bottom) in the absence (solid) and the presence (dotted) of 3.0 mM L-lysine. EPR conditions: $T = 21$ K and $P = 3.2$ mW; enzyme concentrations for top and bottom spectra are 3.7 and 1.8 mg/mL, respectively.

Table 2: Reversible Suppression of the Mn_2 EPR Signals of the Wild-Type Arginase and Mutant Enzymes by L-Lysine

sample	Mn_2 EPR signal (relative amplitude)
(I) wild type + 3.0 mM L-lysine	<0.1
(I) + 1.8 mM L-isoleucine	0.76
(I) + 2.2 mM $B(OH)_3$	0.83
(II) His141Asn + 3.0 mM L-lysine	1.0
(III) His141Asn + 8.9 mM L-lysine	0.97

change in the intensities and resolution of the high-field peaks. Each of the signals exhibits non-Curie temperature dependence of the intensities that fits to a Heisenberg exchange ladder $S = 0, 1, ..., 5$ for a binuclear Mn_2(II,II) site with small negative J values, $|J| < 3.0$ cm^{-1} (Figure S1, panel A, in Supporting Information).

By contrast, L-lysine, which has one additional methylene group in its side chain compared to L-ornithine, acts very differently. This inhibitor causes partial disappearance of the Mn_2(wt) EPR signal at a concentration that inhibits catalytic activity (3.0 mM) (Figure 4, d). The sample was analyzed over a wide range of temperatures from 7 to 150 K, and no new Mn_2 ground or excited state EPR signals, nor free Mn(II), were detected. The effect is reversible upon dialysis to remove L-lysine.

The same concentration of L-lysine (3.0 mM) that eliminates the binuclear Mn_2 EPR signal in wild-type arginase has almost no effect on the Mn_2(His141Asn) mutant EPR signal (Figure 5 and Table 2). A 50% decrease of the Mn_2-(His141Asn) EPR signal could be observed only at much higher concentration of L-lysine (59 mM, not shown), suggesting that the affinity is reduced by at least 20-fold compared to wild-type arginase.

(b) Restoration of the L-Lysine-Suppressed Mn_2(wt) EPR Signal by L-Isoleucine and Borate. Both L-isoleucine and borate are noncompetitive inhibitors of arginase with enzyme−inhibitor dissociation constants of 0.4 mM (*22*) and 1.0 mM (*21*), respectively. Both inhibitors restore the spin-coupled Mn_2 EPR signal in the L-lysine-treated sample (Figure 4, e and f). Addition of 1.8 mM L-isoleucine or 2.2 mM borate to a sample of wild-type arginase, whose Mn_2 EPR signal was suppressed by 90% upon addition of 3.0 mM L-lysine, restores about 80% of the Mn_2 EPR signal intensity (Table 2 and Figure 4). The line shape of these restored Mn_2 signals is similar in shape to original untreated wt sample, except that the ZFS is slightly different.

(c) Interaction with Substrate L-Arginine and N^{ω}-OH-L-Arginine. We were not able to trap intermediates formed upon reaction of wild-type arginase with L-arginine, because the hydrolytic reaction is relatively fast on the time scale of sample mixing [$k_{cat} = 250\ s^{-1}$, pH 9, (*15*)]. In contrast to L-arginine, N^{ω}-OH-L-arginine is hydrolyzed by the wild-type arginase very slowly. It was shown to be a high-affinity, competitive inhibitor with a K_i of 42 μM (*23*). Analogous to L-lysine, N^{ω}-OH-L-arginine reversibly eliminates the binuclear Mn_2(wt) EPR signal. 1.0 mM N^{ω}-OH-L-arginine completely eliminates the signal, leaving only a minor residual mononuclear Mn(II) EPR signal (Figure S2, Supporting Information). The dissociation constant, K_d, of N^{ω}-OH-L-arginine with wild-type arginase was estimated to be about less than 50 μM based on the concentration dependence of the Mn_2(wt) signal. At least 30% of the intensity of the binuclear Mn_2(wt) signal that was suppressed by 1.0 mM N^{ω}-OH-L-arginine could be restored after 12 h dialysis of the enzyme against 25 mM Hepes buffer, pH 7.5 (Figure S2, Supporting Information). Borate addition also accelerates the recovery of the binuclear Mn_2(wt) EPR signal.

No effect of L-arginine on the Mn_2(His141Asn) EPR signal has been found at concentrations lower than 5 mM. A 2-fold decrease in the binuclear Mn_2 EPR signal (with the exception of the central peak at 2700 G) was observed in the presence of a high concentration (70 mM) of L-arginine (Figure S3, Supporting Information). Addition of L-arginine does not change the oxidation state of Mn in arginase. The samples do not change color, nor were oxidized paramagnetic Mn_2-(II,III) or Mn_2(III,IV) species detected by EPR spectroscopy.

A 2−3-fold loss of signal intensity of the Mn_2(His141Asn) signal was observed in the presence of 53 μM N^{ω}-OH-L-arginine, as shown in Figure S4 (Supporting Information). A central six-line component at 3300 G due to a minor mononuclear Mn impurity is not affected. The dissociation constant for loss of the EPR signal was estimated to be 6−18 μM. Therefore, substitution of His141 by Asn preserves the high affinity that the enzyme has for N^{ω}-OH-L-arginine (weak base), in contrast to the considerably reduced affinity for L-lysine and L-arginine (stronger bases). A comparison of the substrate K_m for L-arginine and inhibitor dissociation constants (IC_{50}) for N^{ω}-OH-L-arginine is given in Table 3 for both wild-type and His141Asn mutant proteins.

(d) pH Dependence of Arginase Activity. A study of the rate of substrate hydrolysis was performed over a limited pH range (Table 5). The data show that increasing the pH from 7.5 to 9.0 leads to a decrease of both the K_m value for L-arginine hydrolysis and the K_i value for inhibition of the reaction by L-lysine (Colleluori and Ash, personal communication). The K_i value for L-lysine drops from 6−7 to about 1 mM for wild-type arginase and from 28 to 1 mM for the His141Asn mutant. The K_m value for L-arginine drops from 2.3 to about 1.4 mM for wild-type arginase and from 40 to 19 mM for the His141Asn mutant. The observed pH dependencies for K_m and K_i are consistent with a model for L-arginine hydrolysis that involves deprotonation of the substrate guanidinium group. A wider pH range needs to be examined for the mutant in order to obtain the enzymatic pK_a value for substrate turnover for comparison with the known pK_a for wild-type arginase.

Table 3: Comparison of Substrate Binding (K_m) and Inhibitor Binding, K_d, to Wild-Type and Mutant Arginases

addition	wild type	His141Asn
L-arginine	≈1.5 mM[a]	>40 mM[b]
N^{ω}-OH-L-arginine	<50 μM	<20 μM
L-lysine	<2 mM[b]	>40 mM[b]

[a] K_m for L-arginine hydrolysis (pH 9.0) from ref (*13*). [b] IC_{50} is the concentration that induces 50% suppression of the Mn_2 EPR signal at pH 7.5.

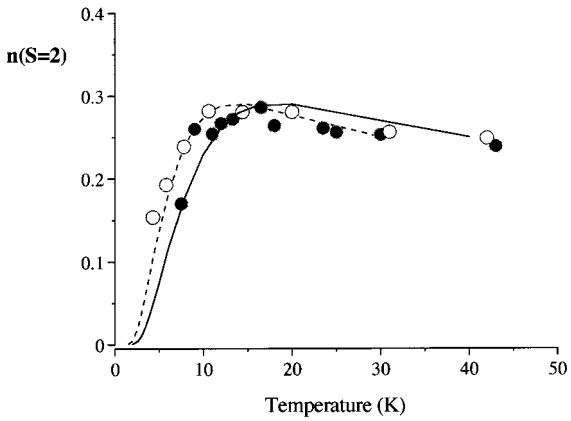

FIGURE 6: Temperature dependencies of the Mn_2 EPR signals of wild-type arginase at pH 9.2 (○) and pH 6.3 (●). Solid (—) and dashed (- - -) curves are the theoretically predicted Boltzmann populations of the quintet state, $n_2(T)$, for a pair of spins $S_A = S_B = {}^5/_2$, coupled by an isotropic Heisenberg interaction $-2JS_AS_B$ with J values of -1.5 and $-2.0\ cm^{-1}$, respectively.

(e) pH Dependence of the Binuclear Mn_2 EPR of WT Arginase. We expected that an increase in pH in the range which activates arginase hydrolytic activity might result in the ionization of the water bridge to hydroxide ion and, therefore, would affect the EPR signals. We found, however, that an increase of pH from 6.3 to 9.2 does not produce any appreciable transformation of the line shape nor the temperature dependence of the Mn_2 EPR signals (Figures 6 and 7). We conclude that although the increase of pH from 6.3 to 9.2 activates arginase (pK_a = 7.5), the solvent bridge does not undergo ionization in this pH region. Hence, a different endogenous base than the μ-solvent must be responsible for the alkaline activation of enzymatic activity Our data support the assignment of His141 as this base.

DISCUSSION

Discrimination between μ-Hydroxo and μ-H_2O Bridging Ligands. Variable-temperature (4−60 K) EPR measurements of wild-type arginase and the His141Asn mutant reveal antiferromagnetic coupling between Mn(II) ions with small

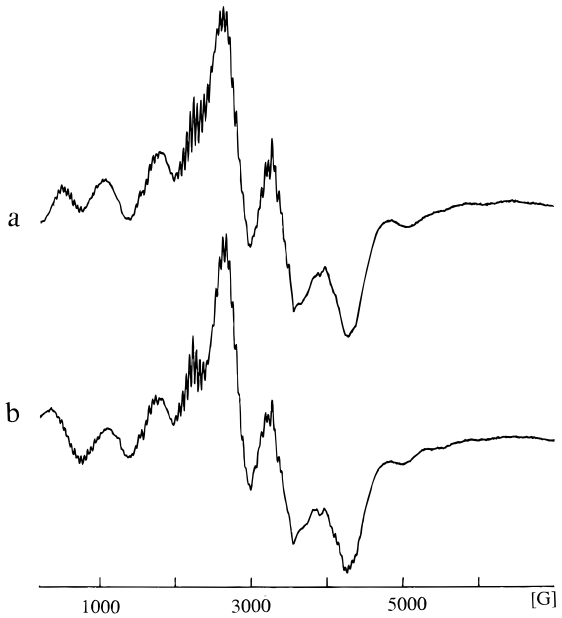

FIGURE 7: Spectra a and b are the binuclear Mn_2 EPR signals of wild-type arginase at pH 7.0 and pH 9.0, respectively. $T = 17$ K; microwave power of 4.1 mW; enzyme concentrations about 26 mg/mL.

J values of -2.0 and -2.5 cm^{-1}, respectively. Relatively small J values, $|J| < 3$ cm^{-1}, were found also for the complexes of wild-type arginase with L-ornithine and L-citrulline, respectively. The accuracy of the fits of the populations used to obtain the J values (20%) precludes values larger than 3 cm^{-1}. For comparison, the temperature behavior of a hypothetical Mn_2(II,II) complex with a J value of -5 cm^{-1} *versus* -2 cm^{-1} is shown in Figure S1, panel B.

For μ-OH- and μ-H_2O-containing Mn_2(II,II) model compounds that also possess one or two O,O′-bridging carboxylate ligands, the strength of the exchange interaction depends on the state of protonation of the bridging oxygen atom in the order $OH^- > H_2O$ (*24*−*27*). The correlation between J and the type of bridging ligand is based on the magnetic properties of the following Mn_2(II,II) compounds with known X-ray structures: $Mn_2(H_2O)(Im)_4(OAc)_4$, $Mn_2(H_2O)_3(F_5C_2COO)_4(L^1)_2$, $Mn_2(H_2O)(L^2)_4(Me_2bipy)_2$, and $Mn_2(H_2O)(OAc)_4(L^3)_2$ with $J = -1.29$, -1.65, -2.73, and -2.95 cm^{-1}, respectively (*24*, *25*, *28*) (here, Im is imidazole, OAc is acetate, L^1 is 2-ethyl-4,4,5,5-tetramethyl-3-oxo-4,5-dihydro-1*H*-imidazolyl-1-oxyl, bipy is bipyridine, L^2 is pivalate, and L^3 is *N*,*N*,*N*′,*N*′-tetramethylethylenediamine). For the μ-OH-containing Mn_2(II,II) compound $Mn_2(OH)(OAc)_2(L^4)_2^+$ (L^4 = *N*,*N*′,*N*″-trimethyl-1,4,7-triazacyclononane), the J value is -9 cm^{-1} (*26*). Three other examples with (μ-acetato)$_{1,2}$ plus μ-phenoxyl or μ-alkoxyl bridges in place of μ-OH fall in the range $J = -3.8$ to -5.5 (*17*). In the only example of a Mn_2(II,II) complex with a single μ-OH bridge and no other bridging atoms, the J value is -2.65 (*29*). If structures are considered with other than μ-carboxylate bridges, then there is more overlap in the range of J values. From this comparison, we see that the small negative J coupling of $|J| < 3$ cm^{-1} for wild-type and mutant arginases is most consistent with a μ-H_2O rather than μ-OH bridge.

This conclusion is further supported by the 2.1 Å resolution X-ray structure of the resting state of arginase, where the Mn−O bond lengths to the bridging solvent molecule were found to be symmetrical at 2.4 Å (*7*). This distance is exceptionally long for a hydroxide bridge [2.05 Å for $Mn_2(OH)(OAc)_2(L^4)_2$](*26*) and hence is best modelled as an unusually long water bridge. The proposed ionization of μ-water to form a μ-hydroxide bridge in this crystalline form of arginase was suggested primarily on the basis of a predicted lower pK_A of 7.2 vs Mn^{2+}_{aq}, which was estimated for the bridging water molecule in an aquo dimer, $[Mn-(H_2O)-Mn]^{4+}_{aq}$, where the Mn−O bond lengths are unknown, but presumed to be shorter than the long distances seen in arginase (*14*).

A recent Mn EXAFS study of wild-type arginase revealed that there was no evidence for detectable Mn...Mn EXAFS scattering, which was interpreted as evidence for the absence of a strongly bound bridging ligand (O^{2-} or OH^-) and in favor of a bridging water molecule (*30*). Taken together, the low $|J|$ value detected in our EPR experiments, the absence of the strong Mn..Mn scattering in EXAFS, and the unusually long Mn−O bond lengths deduced by X-ray diffraction indicate that the bridging solvent molecule in arginase is water, not hydroxide.

The His141Asn Mutation Lowers the Affinity for L*-Lysine and* L*-Arginine.* His141 is not coordinated to either of the Mn ions. It is located in the putative substrate binding channel, between the proposed docking site for the α-aminocarboxylate group at the surface of the protein and 4.5 Å away from Mn_A. Replacement of this residue by Asn was shown to retain a composition of 6 Mn/trimer and to increase by at least 6-fold the K_m value for arginine hydrolysis (*15*).

The present EPR study shows that this mutant also retains an essentially unaltered Mn_2 EPR signal. Neither the line shape (ZFS), the resolved ^{55}Mn hyperfine structure, the spin relaxation rate, nor the inter-manganese exchange interaction differs appreciably from that observed in the wild-type enzyme. Therefore, we conclude that the Mn_2 center of the His141Asn mutant is likely unperturbed compared to that of the wild-type enzyme, shown in Scheme 1.

The Mn_2 center of wild type arginase is essential for the catalase activity (hydrogen peroxide disproportionation) (*14*). The relatively distant location of His141 from the closest Mn ion (≥4.2 Å) may account for the recent observation that the His141Asn mutation does not affect the catalase rate (*31*). Because both the wild-type enzyme and the His141Asn mutant exhibit the same catalase activity, and EPR properties of the Mn_2(II) centers, we concluded that the conserved His141 residue plays no essential role in the catalase activity of arginase. This is somewhat surprising considering the essential need for proton transfer steps during disproportionation of hydrogen peroxide. Presumably, the rate-limiting step in the catalase activity of arginase does not involve transfer of a proton to His141. By contrast, the 10-fold reduction in the rate constant (k_{cat}) of L-arginine hydrolysis by the His141Asn mutant is consistent with His141 functioning as a general base required for catalysis, for example, for deprotonation of the substrate water molecule in eq 1, as suggested by Cavalli et al. (1994). At the same time, the substantially decreased affinity for L-arginine by the His141Asn mutant (Table 3) fully accounts for the increased K_m value for hydrolysis of the mutant *vs* wild-type enzyme (*15*).

EPR Spectroscopy Reveals Two Different Types of Inhibitors. Two different effects on the Mn_2 EPR signal have been observed upon addition of inhibitors to wild-type arginase.

Type 1 inhibitors: L-ornithine, L-citrulline, L-isoleucine, boric acid [$B(OH)_3$], and hydroxylamine (NH_2OH) induce only minor transformation of the line shape of the Mn_2(wt) EPR signal without loss of signal amplitude, suggesting no strong interaction with the Mn_2 center. We propose that these L-α-amino acids may bind to an L-α-aminocarboxylate recognition site on the surface of the protein where inhibition of substrate binding occurs. Borate and hydroxylamine differ structurally from these inhibitors and are presumed to bind to different sites which likewise do not alter the EPR properties. A recent 3 Å resolution X-ray crystallographic study of the inhibition complex between arginase and "boric acid *plus* L-ornithine" reveals that one of the O atoms of the presumed tetrahedral borate anion coordinates the Mn_2 center, probably displacing the bridging aquo ligand between the two Mn ions (*10*). Although an idealized tetrahedral structure for a μ-borate anion was assumed in refining the X-ray model, this could not be distinguished from an asymmetrical Lewis acid complex between a μ-OH^- and boric acid, obtained by ionization of a proton from the μ-H_2O by classical Lewis acid/base chemistry. The resulting μ-HO-$B(OH)_3^-$ anion is electronically analogous to water rather than hydroxide and would be expected to propagate a similar (weak) inter-manganese exchange coupling (J) and zero-field splitting, as is observed. Thus, the EPR data are consistent with the X-ray structure model, suggesting that a μ-HO-$B(OH)_3^-$ anion bridges the Mn pair.

It is also noteworthy that the location of L-ornithine in the X-ray map of the "borate *plus* L-ornithine" complex with arginase places the product outside of the active site channel and well separated from the Mn_2 center (*10*). In agreement with our EPR data, L-ornithine binding induces no loss of the Mn_2 EPR signal intensity, consistent with a weak or outer sphere interaction with the Mn_2 center.

By contrast, L-lysine induces loss of the Mn_2 EPR signal which is related neither to oxidation of the Mn_2 center nor to loss of Mn ions. Subsequent addition of type 1 inhibitors to enzyme preinhibited with L-lysine or N^{ω}-OH-L-arginine restores the binuclear Mn_2 EPR signal, demonstrating that the Mn ions can be restored to a spin-coupled state. Moreover, the binding affinity of N^{ω}-OH-L-arginine is reduced in the presence of type 1 inhibitors, indicating that the two binding sites are competitive, although they produce distinct affects at the Mn_2 center.

The reversible loss of the Mn_2 EPR signal caused by type 2 binders could either be due to an increase in the ZFS from an initial value $|ZFS/gssH| \ll 1$ to ≥ 1 or be due to uncoupling of the Mn ions *via* a decrease of the $|J|$ value, $|J| \leq 0.3$ cm^{-1}. The first mechanism involves an unusually large increase in the ZFS value of the Mn_2(II,II) center, as might be caused by the direct coordination of the terminal *N*-amino group of type 2 inhibitors to the Mn_2 center. A large ZFS value will make the EPR transitions very broad and more difficult to detect by an X-band spectrometer (9.5 GHz). Evidence in support of this interpretation comes from an experiment showing that addition of L-lysine to the His101Asn mutant, which contains only one manganese ion (Mn_B), also induces almost complete disappearance of the EPR signal, as shown in Figure 1, d. This result shows that L-lysine induces an increase of the ZFS value of the Mn_B ion, which could also result, if it were to occur in the case of the wild type arginase, in an increase of the ZFS value of the binuclear Mn_2(II,II) center (*32*). A manuscript describing EPR properties of both the His101Asn and His126Asn mutant enzymes, both containing only one manganese ion, will be published separately (*19*).

A second possible mechanism for loss of the Mn_2 EPR signal intensity involves uncoupling of the Mn electron spins ($J \approx 0$) upon complex formation with type 2 inhibitors. Because the distance between the two Mn(II) ions is relatively small (≤4 Å), only the magnetic dipole−dipole interaction remains following loss of the exchange interaction. The dipolar interaction causes broadening of the EPR signal of the individual Mn(II) ions that is much greater than occurs for the case if J is larger than the dipolar interaction. The magnetic interaction increases in magnitude upon loss of the electron spin exchange interaction because the value of the magnetic moment increases. The average value of $\langle S_z \rangle$ increases upon spin uncoupling of an antiferromagnetic pair of spins. The magnitude of the increase is proportional to $[S_z^2 - {}^1/_3 S(S+1)]$. Hence, for a spin-coupled Mn^{2+} pair, the maximum dipolar interaction in the excited quintet state ($S = 2$, $S_z = 2$) will increase upon uncoupling to form two Mn^{2+} spins ($S = {}^5/_2$, $S_z = {}^5/_2$) by an amount of 13/8. The increase in the dipolar interaction upon spin uncoupling is 3× larger for the triplet state than for the quintet state. Both triplet and quintet states are populated and contribute to the EPR spectrum under the conditions given in Figure 5. If the Mn ions also move upon uncoupling, as is intuitively expected, an additional change in the dipolar interaction is predicted based on the R^{-3} dependence on Mn−Mn distance.

We favor the latter interpretation that the loss of EPR intensity upon binding of type 2 inhibitors is due to spin uncoupling of the Mn ions, resulting from breaking the μ-aquo bridge, possibly by displacing the water molecule to a terminal site on one of the Mn ions (probably Mn_A, because the Mn_B site appears to be more sensitive to binding of substrate), as depicted schematically in Scheme 3. This binding mode differs from that proposed on the basis of inhibitor binding affinities (*9*, *23*) and from modeling of substrate binding to the native enzyme (*7*). Providing more evidence for the geometry and site of substrate/inhibitor binding is a goal of our future studies.

Models for the Strong Inhibition by N^{ω}-OH-L-Arginine. A wide class of L-α-amino acids bearing a side chain with an *N*-OH group in the form of *N*-hydroxyguanidines, amidoximes, and hydroxylamines are known to be strong inhibitors of arginase activity, Table 4 (*9*, *23*).

The distance between the α-carbon and *N*-OH groups appears to be crucial for inhibition by these molecules. N^{δ}-OH-L-Ornithine, for example, is a 37-fold weaker inhibitor of arginase than is N^{ϵ}-OH-L-lysine, differing only by one additional methylene unit in the length of the side chain (*9*). A high inhibitory strength was found for compounds with *N*-OH side chains having their N atom in the same relative position as the side chain as the C^{ϵ} atom of L-arginine. An explanation for the strong inhibition by *N*-OH-containing compounds such as N^{ω}-OH-L-arginine and N^{ϵ}-OH-L-lysine was proposed by Daghigh et al. (1994) and Custot et al. (1996). In both molecules, the geometry and position of the protonated form -NH_2^+-OH side chain groups were proposed

Scheme 3: Schematic View of the Postulated Transition State in L-Arginine Hydrolysis (*7*) (**a**) and Binding of L-N^{ϵ}-OH-Lysine (*9*) (**b**)[a]

a Postulated transition state of L-arginine hydrolysis. Kanyo et al. (1996) *Nature 383*, 554.

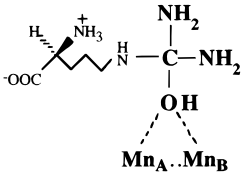

b Proposed binding of L-N^{ϵ}-OH-lysine to the Mn_2 center based on inhibitory study of arginase. Custot et al. (1996) *JBIC 1*, 73.

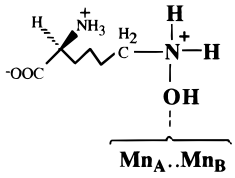

c Proposed coordination of L-lysine based on our EPR data.

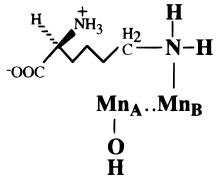

d Proposed coordination of L-N^{ϵ}-OH-lysine.

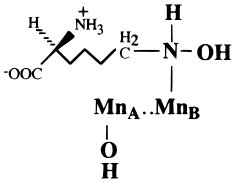

[a] Coordination of the N^{ϵ}-amino group of L-lysine (**c**) and L-N^{ϵ}-OH-lysine (**d**) to Mn_B is proposed on our EPR data.

to be close to the position of the tetrahedral intermediate, resulting from nucleophilic attack of activated water on the C^{ϵ} atom of L-arginine (Scheme 3a,b).

Although structures a and b in Scheme 3 look very similar, it is difficult to reconcile the formation of the μ-(N^{ϵ}-hydroxyl)-bridged species in complex b with the mechanism of the L-arginine hydrolysis proposed by Kanyo et al. (1996) in Scheme 2. Particularly, it is not clear why the weakly basic N^{ϵ} atom of N^{ϵ}-OH-L-lysine (p$K_a \approx 6$) should become protonated upon binding. Moreover, the replacement of μ-aquo in the uninhibited enzyme by a μ-N^{ϵ}-hydroxyl group, with no further alteration of the site, could not lead to spin uncoupling of the Mn(II) ions, in contrast to our results showing loss of the EPR signal.

A Proposed Model for Coordination of L-Lysine, N^{ϵ}-OH-L-Lysine, and N^{ω}-OH-L-Arginine. The EPR data indicate that the N^{ϵ}-amino group of L-lysine could be a direct ligand to the Mn_2 center, particularly to the Mn_B ion. A model that is supported by our data for substrate and inhibitor binding is given in panel c of Scheme 3, where it is compared to two other models. Our model involves deprotonation of the N^{ϵ}-amino group of L-lysine (or N^{ω}-OH-arginine) by transfer to His141 and binding of the neutral *N*-amine atom to Mn_B. Since Mn_B is known from the X-ray structure to have six ligands coordinated to it (*7*), our model requires that one of the ligands must be displaced upon inhibitor binding. Loss of the bridging water ligand is proposed, because this displacement would also account for the disappearance of the EPR signal through the loss of spin exchange coupling.

Table 4: Correlation of the Inhibitor Strength with the Structure of L-Arginine Analogs

Bound molecule	K_i (mM)	pK_a	State of Mn-dimer
No additions			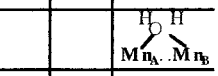
L-arginine (substrate) 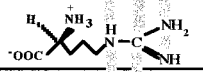	1.0[a]	13.2[b]	
L-N^{ω}-OH-arginine 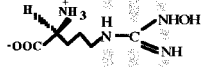	< 0.1[c,d]	8[e]	$Mn_A..Mn_B$
L-citrulline 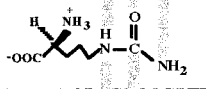	≈ 1.0[d]	0.0[f]	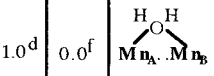
L-N^{ϵ}-OH-lysine 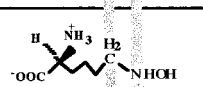	0.004[g]	6[h]	
L-lysine 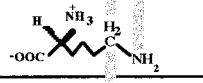	0.9[i]	10.8[b]	$Mn_A..Mn_B$
L-ornithine (product) 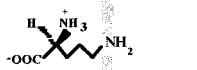	1.0[i]	10.7[b]	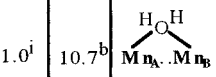
L-N^{δ}-OH-ornithine 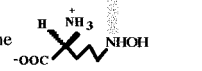	0.15[g]	6[h]	

[a] K_m value for L-arginine hydrolysis at pH 9.0 (*8*, *15*). [b] Ref (*33*). [c] At pH 7.4 (*9*) and at pH 9.0 (*23*). [d] K_d value based on titration of the Mn_2 EPR signal at pH 7.5; this study. [e] Ref (*35*). [f] pK_a for acetylamine (*33*). [g] Bovine liver arginase at pH 7.4 (*9*). [h] pK_a for hydroxylamine (*34*). [i] At pH 9.0 (*8*).

Our model predicts that the difference in binding affinity of L-lysine and N^{ϵ}-OH-L-lysine to arginase is determined by the difference in their proton ionization constants. A correlation exists between the pK_A of the inhibitors and their inhibition constants (Table 4), with stronger binding correlating with the ease of proton ionization. The available data indicate that L-lysine at pH 9.0 and N^{ϵ}-OH-L-lysine at 7.4 are competitive inhibitors of L-arginine hydrolysis with K_i values of 1.0 mM and 4 μM, respectively (*9*, *21*).

$$\text{arginase (L-lysine)} \rightleftharpoons \text{arginase} + \text{L-lysine} \qquad K_i \approx 1.0\ \text{mM, pH} = 9.0$$

When the pH of the buffer solution is lower than the pK_a of L-lysine (10.8), only a minor fraction of deprotonated L-lysine is present:

$$\text{L-lysine}(\text{-}NH_3^+) \rightleftharpoons \text{L-lysine}(\text{-}NH_2) + H^+ \qquad pK_a \approx 10.8$$

The intrinsic inhibition constant, K_i*, can thus be calculated assuming that only the unprotonated form of L-lysine binds to arginase:

$$\text{arginase} + \text{L-lysine}(\text{-}NH_2) \rightleftharpoons \text{arginase [L-lysine}(\text{-}NH_2)] \qquad K_1^* \approx 16\ \mu\text{M}$$

This intrinsic inhibition constant is close to the K_i value for N^{ϵ}-OH-L-lysine also measured under conditions of deprotonation (*36*), suggesting that coordination of the N^{ϵ} atom rather than the hydroxyl group to the Mn_2 center can account for the high affinity of both inhibitors.

Table 5: Effect of pH on K_m and K_i Values for L-Arginine Hydrolysis and Inhibition of This Reaction by L-Lysine, Respectively

	wild-type		His141Asn	
addition	pH 7.5	pH 9.0	pH 7.5	pH 9.0
L-arginine, K_m (mM)	2.3	1.4	19	40
L-lysine, K_i (mM)	6−7	1	28	1

An alternative explanation to consider for the decreased affinity of the His141Asn mutant for L-lysine could be that for some reason the asparagine 141 residue provides an unfavorable condition for coordination of L-lysine. Our experiments with N^{ω}-OH-L-arginine do not support this suggestion. The His141Asn mutant retains a high affinity for N^{ω}-OH-L-arginine (Table 3), indicating that replacement of the histidine residue by asparagine does not play a crucial role in the binding of N^{ω}-OH-L-arginine.

The critical role of His141 as a proton acceptor for substrate binding becomes obvious after comparing the affinities of L-arginine *vs* N^{ω}-OH-L-arginine for the His141Asn mutant. Although the mutant retains a high affinity for the weakly basic N^{ω}-OH-L-arginine molecule, it exhibits greater than 40-fold lower affinity for the extremely basic guanidinium group of L-arginine (Table 3). This is consistent with our previous study indicating a 6-fold decrease of the K_m value for substrate hydrolysis by the His141Asn mutant compared to that of the wild-type arginase (*15*).

Our model predicts that the binding affinity of type 2 inhibitors should be weaker at pH < pK_a (His141) than at pH > pK_a. Although a complete pH dependence has not yet been obtained, the data in Table 5 at pH 7.5 and 9 for inhibition by L-lysine and for substrate hydrolysis (K_i and K_m, respectively) are consistent with a model for L-arginine hydrolysis that involves deprotonation of the substrate guanidinium group or the N^{ϵ}-amine of L-lysine as precursor to binding the side chains of these compounds at the active site.

A recent study has compared the concentration dependence for inhibition of arginase by two new *N*-hydroxyl-type amino acid inhibitors, N^{ω}-OH-nor-L-arginine (nor-NOHA) and homo-NOHA, with two and four CH_2 moieties between the C_{α} atom and *N*-hydroxyl atom, respectively (*36*). These were compared to the inhibitor we have studied here, N^{ω}-OH-L-arginine (NOHA), with three CH_2 moieties. At pH 7.4, the efficiency to inhibit L-arginine hydrolysis was found to decrease with an increase in the number of CH_2 fragments, with IC_{50} values of 2, 40, and 3000 μM for nor-NOHA, NOHA, and homo-NOHA, respectively. These results are consistent with our EPR experiments showing that L-lysine, an inhibitor like nor-NOHA with a five-atom-long side chain length, binds with high affinity to the Mn_2 center, while L-ornithine, with only four atoms in its side chain, binds weakly and not directly to the Mn_2 center. The relatively high inhibitory efficiency of nor-NOHA was attributed to formation of a "nor-NOHA−arginase" complex which imitates the transition state of L-arginine hydrolysis, with the bridging H_2O molecule replaced by the N-hydroxo group, analogous to the proposed structure given in Scheme 3a and related *N*-hydroxo derivatives (*36*, *23*).

Custot et al. (1997) report that the ZFS of the binuclear Mn_2 center was slightly changed upon binding of nor-NOHA, indicating some (weak) interaction (direct or indirect?) with the Mn ions. This behaviour is analogous to the nonbinding type 1 inhibitors described herein. However, they did not report the effect of nor-NOHA on the EPR intensity of arginase. By analogy with N^{ϵ}-OH-L-lysine (K_i = 4 μM), our model predicts that the extremely high inhibitory efficiency of nor-NOHA (K_i = 0.5 μM) (*36*) could be explained by the low pK_a value of its hydroxyguanidinium group, thereby creating a higher concentration of the neutral (unprotonated) form that is necessary for high-affinity binding. Like other type 2 inhibitors, the uncharged form of the side chain has no charge constraints and can gain access to the Mn_2 site. We propose that nor-NOHA binds directly to the Mn_2 site by coordination of the N^{ω} atom to Mn_B and breaking of the μ-aquo bridge, like the other type 2 inhibitors. This contrasts with the proposal by Custot et al. (1997), who attribute the high-affinity binding to the formation of the μ-hydroxy bridging geometry, analogous to Scheme 3a. To sort this difference out, both labs need first to compare the EPR properties of arginase inhibited by the same inhibitors.

A New Proposal for the Mechanism of Hydrolytic Cleavage of L-Arginine. A new mechanism for catalysis by arginase based on our EPR studies is depicted in Scheme 4.

(1) The first step involves entry of protonated L-arginine-(H^+) into the active site region by transfer of the guanidinium proton to His141 and binding of the terminal imino N atom to Mn_B. There is compelling chemical evidence from model complexes that the neutral guanidine ligand prefers to coordinate to both hard and soft metal ions *via* ligation of the terminal imino NH and not the amino NH_2 group by at least 10-fold higher probability (*37*). Analogous to the binding of L-lysine and N^{ω}-OH-L-arginine, we propose that L-arginine also binds like a type 2 inhibitor, causing loss of inter-manganese electronic coupling by breaking of the μ-aquo bridge and increasing the inter-manganese distance. We hypothesize that breaking the μ-aquo bridge is facilitated by a "carboxylate shift" (*38*) of the monodenate $\mu_{1,1}$-Asp232 bridge to the O,O′ bridging mode.

(2) The second step involves proton transfer from the aquo ligand on Mn_A to the most basic amine site on the substrate, the N^{δ}-guanidino atom. This step also forms a nucleophilic hydroxide ion bound to a single Mn ion. Protonation of the N^{δ}-guanidino atom should be assisted by the close proximity of the negatively charged carboxylate group of the Glu277 which has O and O′ atoms separated from Mn_B by 6.7 and 5.6 Å in the unliganded structure. This position places the anionic carboxylate of Glu277 juxtaposed to the cationic -$N^{\delta}H_2$- group of L-arginine in the proposed mechanism. Here is where we can understand the reason why arginase favors having μ-aquo instead of μ-hydroxide, as it requires breaking of a weaker Mn−μ-aquo bond. Step 2 in this mechanism would have to be modified slightly if the reactive form of the enzyme contains the μ-hydroxide bridging conformer instead of the μ-aquo form deduced herein. In this case, breaking of the stronger Mn−μ-hydroxide bond upon substrate coordination to Mn_B moves the nucleophile hydroxide to Mn_A without need for further proton transfer. In this case, protonation of the substrate N^{δ} atom must occur at a later stage in the mechanism from a different proton donor than the μ-aquo [possibly His(H^+)141].

Scheme 4: Model of L-Arginine Hydrolysis Based on This Work

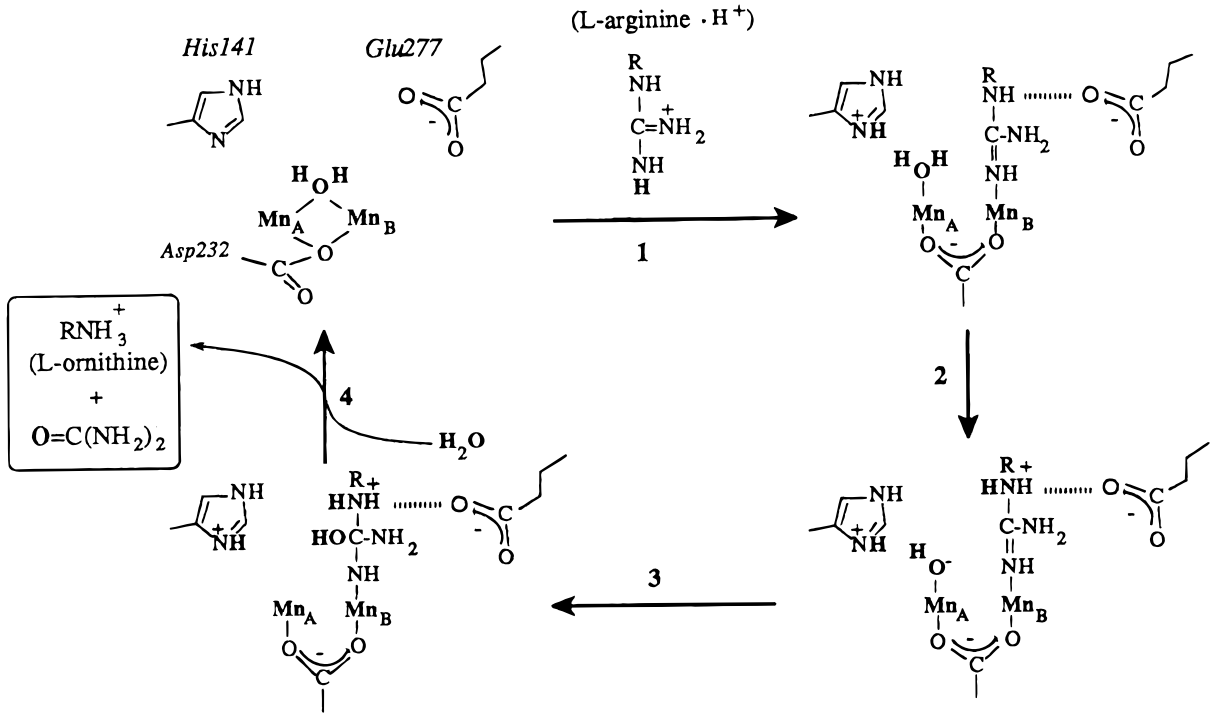

(3) The third step involves dissociation of hydroxide from Mn_A and attack at the guanidinium carbon atom to form a tetrahedral intermediate. This step should be driven by the highly electrophilic character of the guanidinium carbon caused both by coordination of its terminal imino N atom to Mn_B and by protonation of the N^{δ} atom.

(4) The catalytic cycle is completed by collapse of the tetrahedral intermediate by cleavage of the $C^{\epsilon}-N^{\delta}$ bond initiated by transfer of the second proton to N^{δ}, forming the products L-ornithine(H^+) and coordinated urea. Release of L-ornithine(H^+) can occur immediately, while release of urea occurs by proton transfer from His141, thereby restoring the resting state. This sequence is consistent with the inhibitory studies of Reczkowski and Ash (1994) and Sossong et al. (1997).

The above mechanism proposes intermediates that have plausible chemical precedent in model complexes (*37*, *39*, *40*). It also shares features in common with the mechanisms of several other binuclear metallohydrolases (*11*, *12*), including hydrolysis of urea by urease [Ni_2(II,II) site], phosphate ester hydrolysis by purple acid phosphatases [containing an Fe(III)−Zn(II) center], and phosphoprotein hydrolases like calcineurin, among several others. There are two important features of this mechanism that we believe may have general applicability to other binuclear hydrolases. First, although μ-aquo bridges are predicted to have lower pK_A values than terminal aquo ligands, thereby increasing their concentration, they are not necessarily good nucleophiles unless there is a mechanism for dissociation or first converting them to kinetically more accessible terminal sites. Second, this required activation of the nucleophile could be achieved by coupling substrate binding at one metal ion to dissociation of the μ-aquo bridge, forming the kinetically accessible hydroxide, as illustrated in our model.

To our knowledge, there is no demonstrated evidence in any chemical system for μ-aquo, -hydroxo, or -oxo atom bridges between metal ions functioning directly as a nucleophile in any hydrolysis reaction, without first breaking one of the M−OH bonds. On the other hand, there is compelling evidence that terminal hydroxide ligands in bimetallic complexes do function as efficient nucleophiles for hydrolysis of peptide and phosphate esters (*39*−*41*) and triphosphate esters (*42*). The available evidence indicates that metal-bridging hydroxo ligands are not sufficiently strong nucleophiles because they are bound to two electropositive metal ions, using two lone pairs of electrons that are unavailable for initiating nucleophilic hydrolysis reactions (*11*). However, if the μ-hydroxide can be released by coupling to substrate binding, a strong nucleophile is unleashed in the majority of centers.

Our mechanism for catalysis by arginase differs in several important aspects from the recent proposal based on modeling of the possible nonbonded interactions of L-arginine to native enzyme (*7*) in the following ways: (1) the binding of substrate L-arginine to Glu277 and not to either Mn ion; (2) the His141 residue is not involved in deprotonation of the substrate or inhibitors upon binding; and (3) in the critical bond-forming step the (nonnucleophilic) bridging μ-hydroxide ion is proposed to attack the guanidinium carbon to form a trivalent μ_3-oxo bridge.

ACKNOWLEDGMENT

We thank D. Colleluori for measurements of the hydrolytic activity of wild-type and mutant arginase.

SUPPORTING INFORMATION AVAILABLE

Four figures illustrating temperature dependencies of the EPR signals of L-ornithine- and L-citrulline-treated wild-type arginase, the effect of L-arginine on the His141Asn mutant, and the effect of N^{ω}-OH-L-arginine on wild-type arginase

and the His141Asn mutant (6 pages). Ordering information is given on any current masthead page.

REFERENCES

1. Abdelal, A. T. (1979) *Annu. Rev. Microbiol. 33*, 139−168.
2. Cunin, R., Glansdorff, N., Pierard, A., and Stalon, V. (1986) *Microbiol. Rev. 50*, 314−352.
3. David, R. H. (1986) *Microbiol. Rev. 50*, 280−313.
4. Hellerman, L. A., and Perkins, M. E. (1935) *J. Biol. Chem. 112*, 175−194.
5. Hellerman, L. A. (1937) *Physiol. Rev. 17*, 454.
6. Penninckx, M., Simon, J.-P., and Wiame, J.-M. (1974) *Eur. J. Biochem. 49*, 429.
7. Kanyo, Z. F., Scolnick, L. R., Ash, D. E., and Christianson, D. W. (1996) *Nature 383*, 554−557.
8. Reczkowski, R. S., and Ash, D. E. (1992) *J. Am. Chem. Soc. 114*, 10992−10994.
9. Custot, J., Boucher, J.-L., Vadon, S., Guedes, C., Dijols, S., Delaforge, M., and Mansuy, D. (1996) *JBIC, J. Biol. Inorg. Chem. 1*, 73−82.
10. Baggio, R., Elbaum, D., Kanyo, Z. F., Carroll, P. J., Cavalli, R. C., Ash, D. E., and Christianson, D. W. (1997) *J. Am. Chem. Soc. 119*, 8107−8108.
11. Dismukes, G. C. (1996) *Chem. Rev. 96*, 2909−2926.
12. Wilcox, D. E. (1996) *Chem. Rev. 96*, 2435−2458.
13. Pontius, B. W., Lott, W. B., and von Hippel, P. H. (1997) *Proc. Natl. Acad. Sci. U.S.A. 94*, 2290−2294.
14. Sossong, T. M., Khangulov, S. V., Cavalli, R. C., Soprano, D. R., Dismukes, G. C., and Ash, D. E. (1997) *JBIC, J. Biol. Inorg. Chem. 2*, 433−443.
15. Cavalli, R. C., Burke, C. J., Soprano, D. R., Kawamoto, S., and Ash, D. E. (1994) *Biochemistry 33*, 10652−10657.
16. Khangulov, S. V., Sivaraja, M., Barynin, V. V., and Dismukes, G. C. (1993) *Biochemistry 32*, 4912−4924.
17. Khangulov, S. V., Pessiki, P. J., Barynin, V. V., Ash, D., and Dismukes, G. C. (1995) *Biochemistry 34*, 2015−2025.
18. Baranowski, J., Cukierda, T., Jezowska-Trzebiatowska, B., and Kozlowski, H. (1979) *J. Magn. Reson. 33*, 585−593.
19. Khangulov, S. V., Sossong, T. M., Ash, D. E., and Dismukes, G. C. (unpublished results).
20. Campbell, J. W. (1966) *Comp. Biochem. Physiol. 18*, 179.
21. Reczkowski, R. S., and Ash, D. E. (1994) *Arch. Biochem. Biophys. 312*, 31−37.
22. Carvajal, N., and Cederbaum, S. D. (1986) *Biochim. Biophys. Acta 870*, 181.
23. Daghigh, F., Fukuto, J. M., and Ash, D. E. (1994) *Biochem. Biophys. Res. Commun. 202*, 174−180.
24. Caneschi, A., Ferraro, F., Gatteschi, D., Melandri, M. C., Rey, P., and Sessoli, R. (1989) *Angew. Chem., Int. Ed. Engl. 28*, 1365−1367.
25. Yu, S.-B., Lippard, S. J., Shweky, I., and Bino, A. (1992) *Inorg. Chem. 31*, 3502−3504.
26. Bossek, U., Wieghardt, K., Nuber, B., and Weiss, J. (1989) *Inorg. Chim. Acta 165*, 123−129.
27. Wieghardt, K., Bossek, U., Nuber, B., Weiss, J., Bonvoisin, J., Corbella, M., Vitols, S. E., and Girerd, J. J. (1988) *J. Am. Chem. Soc. 110*, 7398−7411.
28. Schultz, B., Ye, B.-H., Li, X.-Y., and Chan, S. I. (1997) *Inorg. Chem. 36*, 2617−2622.
29. Flassbeck, C., Weigardt, K., Bill, E., Butzlaff, C., Trautwein, A. X., Nuber, B., and Weiss, J. (1992) *Inorg. Chem. 31*, 21−25.
30. Stemmler, T. L., Sossong, T. M., I., G. J., Ash, D. E., Elgren, T. E., Kurtz, D. M. J., and Penner-Hahn, J. E. (1997) *Biochemistry 36*, 9847−9858.
31. Sossong, T. (personal communication).
32. Owen, J., and Harris, E. A. (1972) in *Electron Paramagnetic Resonance* (Geschwind, S., Ed.) pp 427−492, Plenum Press, New York.
33. Streitwieser, A., Heatcock, C. H., and Kosower, E. M. (1992) *Introduction to organic chemistry*, Fourth ed., 520, Macmillan Publishing Co., New York.
34. Shriver, D. F., Atkins, P., and Langford, C. H. (1994) *Inorganic chemistry*, p 519, W. H. Freeman, New York.
35. Everett, S. A., Dennis, M. F., Patel, K. B., Stratford, M. R., and Wardman, P. (1996) *Biochem. J. 317*, 17−21.
36. Custot, J., Moali, C., Brollo, M., Boucher, J. L., Delaforge, M., Mansuy, D., Tenu, J. P., and Zimmermann, J. L. (1997) *J. Am. Chem. Soc. 119*, 4086−4087.
37. Fairlie, D. P., Jackson, W. G., Skelton, B. W., Wen, H., White, A. H., Wickramasinghe, W. A., Woon, T. C., and Taube, H. (1997) *Inorg. Chem. 36*, 1020−1028.
38. Rardin, R. L., Tolman, W. B., and Lippard, S. J. (1991) *New J. Chem. 15*, 417−430.
39. Chin, J. (1991) *Acc. Chem. Res. 24*, 145−152.
40. Duboc-Toia, C. S., Ménage, J.-M., Vincent, M.-T., Averbuch-Pouchot, and Fontecave, M. (1997) *Inorg. Chem. 36*, 6148−6149.
41. Rawlings, J., Hengge, A. C., and Cleland, W. W. (1997) *J. Am. Chem. Soc. 119*, 542−549.
42. Sigel, H. (1990) *Coord. Chem. Rev. 100*, 453−539.

BI972874C